

## Q-statistics in dynamic speckle pattern analysis

Héctor J. Rabal<sup>a,\*</sup>, Nelly Cap<sup>a</sup>, Marcelo Trivi<sup>a</sup>, Marcelo N. Guzmán<sup>a,b</sup>

<sup>a</sup> Centro de Investigaciones Ópticas (CONICET La Plata-CIC), UID Optimo, Departamento de Ciencias Básicas, Facultad de Ingeniería, Universidad Nacional de la Plata, P.O. Box 3, 1897, Gonnet, La Plata, Argentina

<sup>b</sup> Laboratorio Láser, Facultad de Ingeniería, Universidad Nacional de Mar del Plata, Juan B. Justo, 4302, 7600 Mar del Plata, Argentina

### ARTICLE INFO

#### Article history:

Received 20 November 2011

Received in revised form

11 January 2012

Accepted 12 January 2012

Available online 1 February 2012

#### Keywords:

Tsallis statistics

Dynamic speckle

### ABSTRACT

We introduce  $q$  statistics concepts to improve the performance of some methods based on the histogram to estimate dynamic speckle activity. It is shown that some improvements are obtained by choosing appropriate  $q$  values that have been empirically determined. The possibility of increasing the precision and diminishing the acquisition time are explored for a usual study case as is the drying of paint.

© 2012 Elsevier Ltd. All rights reserved.

### 1. Introduction

In 1988 Tsallis [1] extended the domain of validity of standard thermodynamics and Boltzmann–Gibbs (B–G) statistical mechanics in order to cover a variety of anomalous systems. Systems involving long range interactions, long range microscopic memory in non-markovian stochastic processes, pure electron–plasma two dimensional turbulence, phonon–electron anomalous thermalization in ion-bombarded solids, solar neutrinos, etc. are some examples where the B–G theory presents difficulties. To overcome at least some of these problems, Tsallis' formalism proposed the extension of the concept of entropy by including a free parameter  $q$  to give origin to what is called *non extensive statistics*. This generalization proved to be very fruitful and, aside from thermodynamics, it was successfully applied to a wide variety of phenomena and to further generalizations including  $q$  parameter versions of several functions and operators (named  $q$  deformed algebra) such as  $q$  Gaussian,  $q$  mean value,  $q$  exponential,  $q$  logarithm, etc.

Some general properties of Tsallis entropy  $S_q$  are:  $S_q$  is positive, takes zero value for absolute certainty and increases monotonously with increasing uncertainty.

The generalization found interesting applications in widely different (some perhaps unexpected) fields. It has been applied to both theoretically well founded situations and experimental ones. A somewhat random view includes the order of words in a text, the citation of scientific papers, electroencephalography signals of epilepsy, to monitor brain injury after cardiac arrest, in financial

markets, seismicity, atmospheric turbulence, gravitation, etc. An extended review of these subjects was presented in Refs. [2,3]. In image processing it has been applied to image registration, image thresholding, segmentation of cerebral tissue in multiple sclerosis magnetic resonance images, etc.

In optics, the study of the speckle patterns, due to their random nature, requires using statistical tools, the properties of which depend on the coherence of the incident light and the characteristics of the diffusing surface [4]. In the case of living samples and in some industrial processes, speckle patterns evolve in time and the dynamic speckles have different characteristics that can be used to obtain information on the phenomena participating in its origin [5].

In dynamic speckle metrology, where different statistic tools are required, some improvements in the measurements of activity, based on the histogram, could be expected by exploring different  $q$  values. However, the choice of the  $q$  value will be then dependent on the investigated phenomenon and the type of measurement.

In this work, we analyze some aspects of the statistical properties of dynamics speckle patterns using the Tsallis  $q$  formalism. We test  $q$  statistics adapted to that end to find the best suited values of the  $q$  parameter that optimize the application of several usual measurement algorithms in dynamic speckle. The improvements are, in some cases, rather subtle.

For  $q=1$  the classic results are obtained; small (close to zero)  $q$  values emphasize the weight of rare events of the intensity histogram while high values of  $q$  emphasize the effect of frequent events. Since the effect of the variation of  $q$  is to change the balance between rare and frequent events, the improvements are in some cases rather subtle.

\* Corresponding author. Tel.: +54 221 484 2957; fax: +54 221 471 2771.  
E-mail address: [hrabal@ing.unlp.edu.ar](mailto:hrabal@ing.unlp.edu.ar) (H.J. Rabal).

We present a brief description of the Tsallis  $q$  formalism and review some algorithms for the characterization of dynamic speckle patterns. Then,  $q$  mean value,  $q$ -entropy,  $q$ -standard deviation, LASCA $q$ , a  $q$  variation of the inertia moment of the co-occurrence matrix and the Briers temporal contrast (BTC) are tested. We use a numerical simulation and a classic study of the drying of paint process. This is a well known process, the behavior of which is adequately characterized by dynamic speckle patterns [6]. The numerical simulation was used only in the technique (BTC) where experimental data could not be obtained and a well based theoretical basis already existed.

The  $q$  values in the 0, 1 interval were tested and it was found that some of these tools perform better when used with adequately chosen  $q$  values, as well as  $q$  values greater than 1 which we also tested. Values of  $q$  greater than 1 did not show any appreciable improvement in the tested cases. By adequately chosen values of  $q$  we mean that when those values are used, resolution is better or standard deviation is smaller, etc.

## 2. Theory

We work with dynamic speckle processes [7]. In the case where the sample shows a similar behavior all over its surface it is possible to study it with a single image obtained in a free propagation experimental device using objective speckles. This geometry provides a large amount of data describing simultaneously the same physical situation as contributions of the scattered light that are collected by every pixel of the detector. So, every pixel in the CCD camera provides a simultaneous measurement of the dynamics.

Conversely, if it is necessary to screen regions of the surface that show similar behavior, then an image forming configuration, named subjective speckle patterns, is required, and eventually many images might be needed to follow the time evolution of the intensity in each separate pixel to obtain significant statistics. As the processing with  $q$  statistics requires the use of the intensity histogram, for the results to be different from classical quantities ( $q=1$ ) a higher number of samples is necessary. The sampling rate should then be faster than the explored phenomenon and it should be assumed stationary during the acquisition of the images.

Of course, the grabbing and processing of a single image is faster, and for fast phenomena this configuration might be the only adequate one. In what follows, we are going to refer them to the histogram of a spatial distribution obtained from a dynamic speckle pattern sample by free propagation.

### 2.1. $q$ -mean value

To apply the  $q$  formalism in dynamic speckle techniques, following [2] we call  $q$ -mean value of a certain magnitude  $A$ :

$$\langle A \rangle_q \equiv \frac{1}{S} \sum_{i=1}^W p_i^q A_i \quad (1)$$

where  $p_i$  is the probability of the  $A_i$  value,  $q$  is called the parameter of non-extensivity and  $W$  is the number of possible values of the magnitude  $A$ .  $S$  is a normalization value defined as

$$S = \sum_{i=1}^W p_i^q \quad (2)$$

To calculate  $q$ -mean value, first the histogram of the intensity  $I$  is constructed. From the histogram the probabilities  $p_i$  are determined and the  $q$  mean value is calculated using Eq. (1) and using the intensity  $I$  as the magnitude  $A$ . This first step is a mapping of the ordinary normalized histogram  $H(i)$  by raising

every value of it to the  $q$  power and dividing by the normalizing factor. Fig. 1 shows an example of the result of this operation for three different  $q$  values: (a)  $q=1$ , (b)  $q=0.05$  and (c)  $q=3$ . For  $q=1$  the histogram is not modified and the classic mean value is obtained. For  $q < 1$  this operation has the effect of comparatively increasing the value of the probability of rare events. The modified histogram  $H_q(i)$  is then more even, thus resulting in an increase of the classical entropy. For  $q > 1$  the converse is true; frequent values are emphasized and classical entropy decreases.

The resulting  $H_q(i)$  is then used for the calculation of  $q$  versions of other statistical measures used in dynamic speckle that are defined next.

### 2.2. $q$ Variance

The  $q$ -Variance  $\sigma_q^2$  is defined here as the  $q$  mean value of  $(I - \langle I \rangle_q)^2$ .

$$\sigma_q^2 = \left\langle (I - \langle I \rangle_q)^2 \right\rangle_q \quad (3)$$

where  $I$  is the intensity.

### 2.3. LASCA (laser contrast speckle analysis)

LASCA [8] is an almost real time and non-scanning technique that uses the spatial first order statistics of time integrated speckle. It is used to build images to measure blood perfusion.

If intensity variations are relatively fast, finite integration time causes the (spatial) standard deviation  $\sigma_{x,y}$  of the measured intensity  $I$  variations to diminish and so does the contrast defined as

$$C = \frac{\sigma_{x,y}}{\langle I \rangle} \quad (4)$$

where  $\langle I \rangle$  is the spatial average of the intensity. This magnitude is a measure of the degree of blur exhibited by the diagram.

As  $C$  diminishes with increased activity and blur, an image constructed on this basis shows reversed contrast; with its active places appearing in dark regions and conversely. As a spatial standard deviation is required, the operation is calculated on spatial windows and involves some reduction in resolution. It is widely used in medicine applications [9].

LASCA with  $q$  values is defined as

$$C_q = \frac{\sigma_q}{\langle I \rangle_q} \quad (5)$$

where mean values and standard deviations are calculated using Eqs. (1) and (3), on time integrated speckle pattern spatial statistics.

In a spatial window for classical LASCA ( $q=1$ ) there are few values (usually  $3 \times 3$ ,  $5 \times 5$ , or  $7 \times 7$  square pixels windows) as these windows are kept small to maintain the maximal spatial resolution. So, in general there will be few repetitions and the histogram will be very poor. There will be very few frequent values. Most of them will appear only once. If all the values are different (the most probable situation) then all the  $q$  powers of the  $p_i$  are the same for all  $q$ , so that in mean value calculations the value  $p_i$  appears as a common factor that can be taken out of the sum and cancels with the same value in the normalization denominator. All events are then equally frequent and the result is the same as with ordinary ( $q=1$ ) LASCA. Something similar happens if all the values inside the window are the same.

Then, the result only differs from ordinary LASCA if some value appears more than once in the histogram and that variation is small unless  $q$  is very different from 1. Then, unless the window is big the result will be very similar to LASCA.

A big window is a serious limitation to image spatial resolution. It also requires that all the pixels inside it represent the same

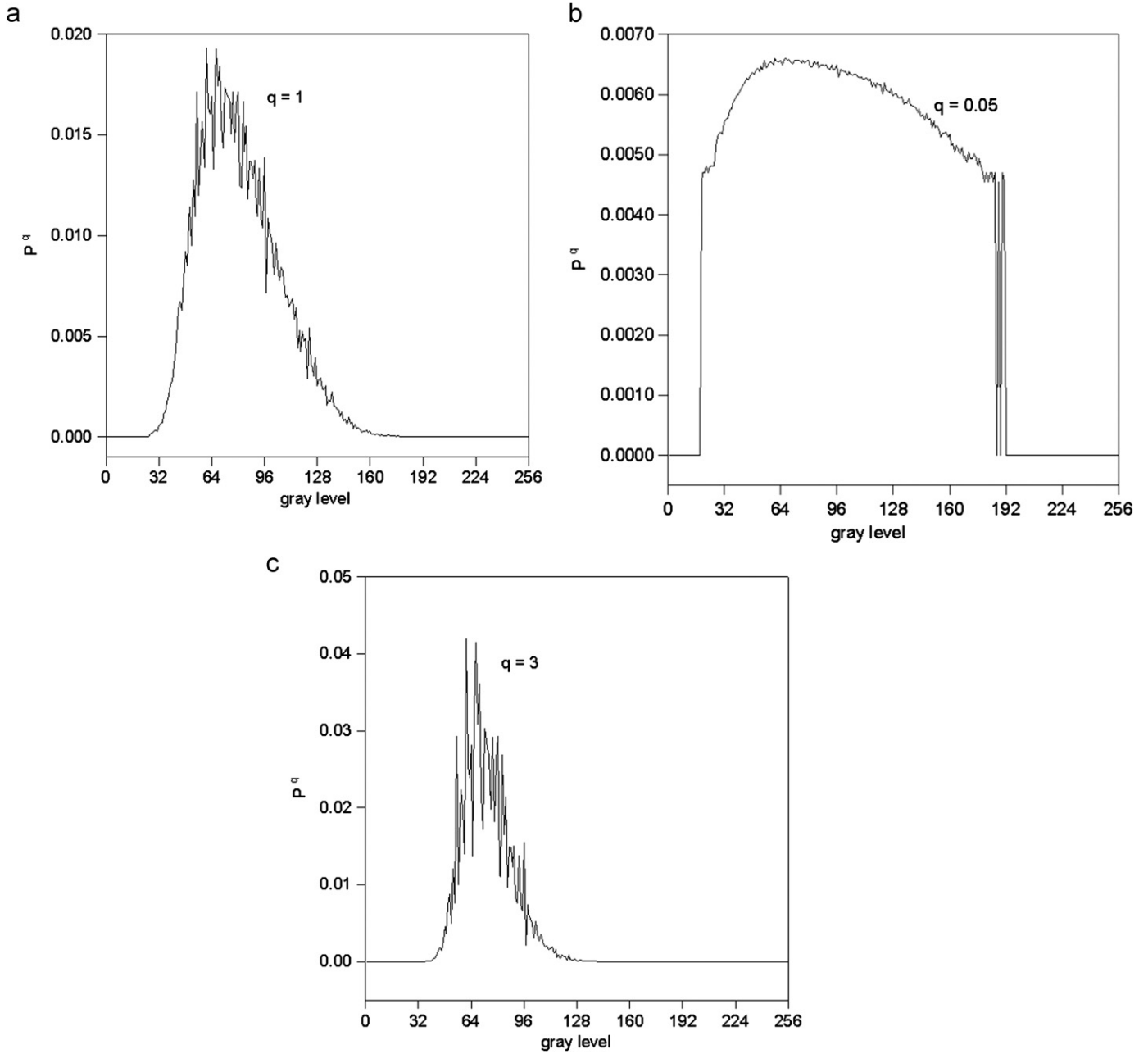


Fig. 1. Normalized probabilities for three different  $q$  values: (a)  $q=1$ , (b)  $q=0.05$  and (c)  $q=3$ . Notice the different scales of the ordinates.

physical situation. Then the speckle pattern must be obtained by free propagation (objective speckles). The result is then a single number and not an image for each  $q$  value.

The choice of the value of  $q$  is free and can be used to calculate a function: *LASCA- $q$*  as a function of  $q$ . It requires only a single frame of a dynamic speckle pattern.

2.4. Tsallis entropy and  $q$  parameter

$S_q$  is the  $q$ -entropy defined by Tsallis [1] is

$$S_q = k \frac{1 - \sum_{i=1}^W p_i^q}{q-1} \tag{6}$$

where  $k$  is a positive constant. It reduces to the classical Boltzmann–Gibbs entropy in the limit when  $q \rightarrow 1$ .

2.5. Inertia moment of the Co-occurrence matrix

The Co-occurrence matrix (COM) of a set of frame consecutives in time, called the Temporal History of the Speckle Pattern (THSP) [10], is defined as a matrix where the entries are the number  $N_{ij}$  of occurrences of a certain intensity value  $i$ , that is immediately followed in time by an intensity value  $j$ . It is

$$COM = [N_{ij}] \tag{7}$$

For normalization purposes, it is convenient to divide each row of this matrix by the number of times that the first gray level appeared.

$$p_{ij} = \frac{N_{ij}}{\sum_j N_{ij}} \tag{8}$$

Then the sum of the components in each row equals 1.

A measurement of the spread of the COM values around the principal diagonal with these features can be constructed as the sum of the matrix values times its squared row distance to the principal diagonal [10]. This is a particular second order moment called the Inertia Moment ( $IM$ ) of the matrix with respect to its principal diagonal in the row direction. So inertia moment ( $IM$ ) is defined as

$$IM = \sum_{ij} p_{ij}(i-j)^2 \quad (9)$$

where  $i, j$  are intensity levels and  $p_{ij}$  are the time transition probabilities of those levels.

This concept is now generalized to the  $q$  statistic of Inertia Moment ( $IM_q$ ) as follows:

$$IM_q = \sum_{ij} p_{ij}^q (i-j)^2 \quad (10)$$

This result most also be divided by  $S$  as in Eq. (2) for normalization purposes.

### 2.6. Briers's temporal contrast

There is a time contrast measure that was proposed by Briers [11]  $B = \frac{\langle \sigma_t^2(x,y) \rangle}{\langle I \rangle^2}$  where  $\langle \rangle$  indicates spatial ensemble average and  $\sigma_t$  is the standard deviation with respect to time at pixel  $(x,y)$ .

It theoretically relates the proportion  $\rho$  of moving to total number of scattering centers in the illuminated sample as

$$\rho = 1 - \left[ 1 - \frac{\langle \sigma_t^2(x,y) \rangle}{\langle I \rangle^2} \right]^{1/2} \quad (11)$$

This relationship agrees very well with numerical simulations [12], when these classical definitions of mean value and standard deviation are employed.

The definition of  $B$  can be generalized to include a parameter  $q$  by replacing both  $\sigma_t^2$  and  $\langle I \rangle$  by their  $q$  versions as in Eqs. (1) and (3).

$$B_q = \frac{\langle (\sigma_t^2)_q \rangle_{x,y}}{\langle I_q \rangle^2} \quad (12)$$

where the subscript  $x,y$  indicates ordinary spatial average.

## 3. Experiments and results

In this section we are going to show examples where the proposed  $q$  formalism is applied to the case of the study of dynamic speckle patterns in an experimental situation. It concerns the following of the drying of paint process which is a well known example where the evolution of the speckle patterns [6] carries out the analysis that reproduces very well drying curves. We are then going to use it as a test for the application of the algorithms to analyze its performance.

This process had been previously analyzed using dynamic speckle and was compared with the weight loss of the sample [6]. The results obtained from the optical and the gravimetric measurements show that the activity over the whole sample decreases monotonically with time as the solvent is evaporated. Fig. 2 shows the experimental set up. White water-borne paint films were applied onto a  $4 \times 4 \text{ cm}^2$  of glass substrate using a standard drawdown  $150 \mu\text{m}$  applicator. An attenuated unexpanded  $10 \text{ mW}$  He-Ne laser was used to illuminate the sample. A lensless CCD camera Pulnix TM-6CN (cell size  $8.6 \text{ (H)} \times 8.3 \text{ (V)}$  microns) connected to a personal computer with a frame grabber was used to record the images that were digitized to 256 intensity levels

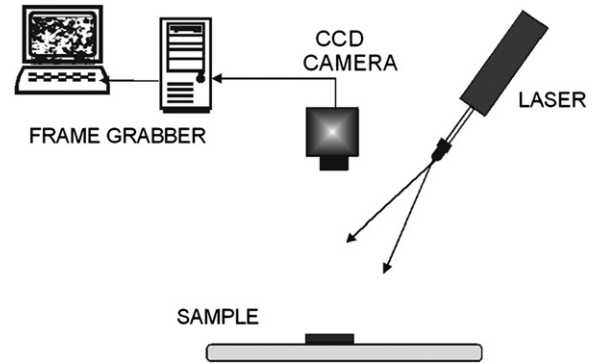


Fig. 2. Experimental set up used to acquire objective speckle pattern sequences.

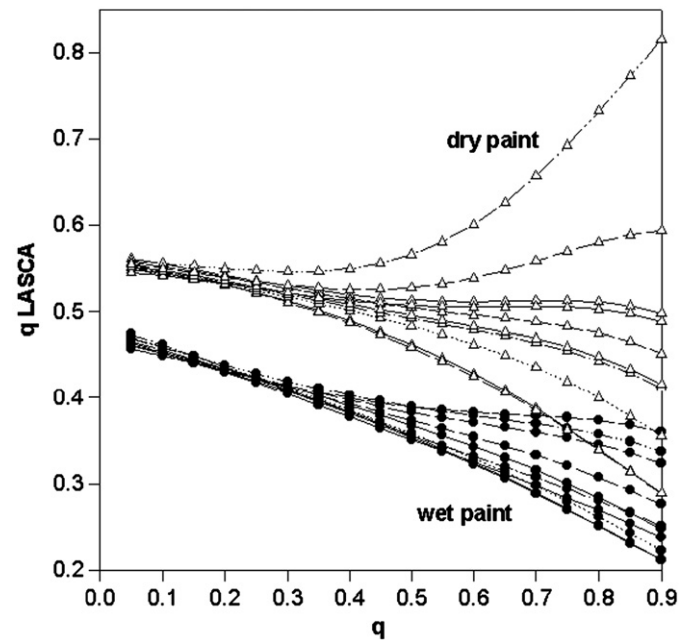


Fig. 3. LASCA  $q$  statistics for a speckle pattern obtained with 10 different frames of wet and almost dry paint. For  $q$  near to 1, wet and dry states overlap. Small  $q$  values considerably reduce the spread and both states can be differentiated.

(8bits). The speckles were well resolved by the CCD sensor and the average intensity of the laser was maintained constant.

Different  $q$ -algorithms were employed to analyze the drying of paint process experiment.

The LASCA method, involving a single frame, although giving good results in blood flow measurement is not a good descriptor in some other dynamic phenomena (the paint drying phenomenon, for example). However, the reformulated LASCA $q$  algorithm for  $q \neq 1$  shows a noticeable improvement for the description of the drying of paint experiment.

The successive steps for this calculation were:

We used each frame obtained of the dynamic speckle produced by fresh paint, for example. The intensity histogram of this frame was calculated, and with it, the normalized probability distribution for each  $q$  value was calculated. An example is shown in Fig. 1. Then, the  $q$  mean value was calculated as in Eq. (1) and its  $q$  standard deviation using the square root of Eq. (3). LASCA $q$  was then obtained using Eq. (5) and the results plotted for different  $q$  values.

Fig. 3 shows the result of using LASCA with  $q$  statistics for a speckle pattern obtained with fresh and almost dry paint. It can be seen that for  $q$  near to 1 the results obtained with the repetition of the same experiment show a very high spread and

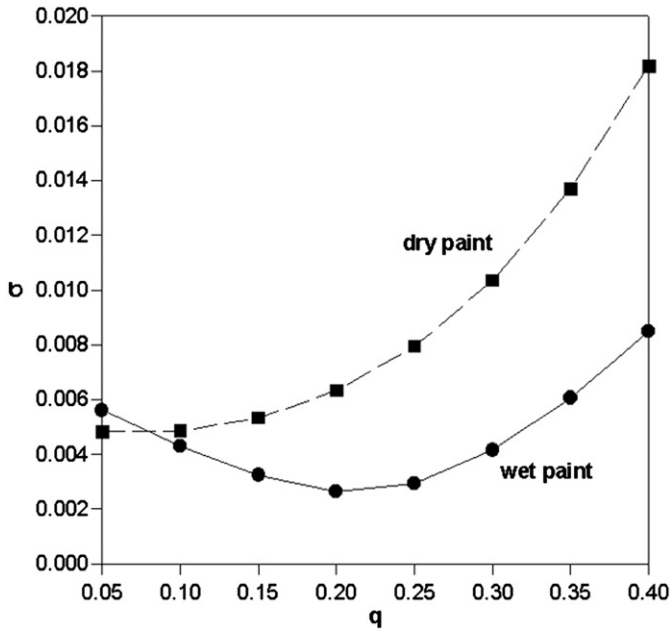


Fig. 4. Standard deviation of the 10 LASCAq measurements corresponding to Fig. 3. A minimum value is registered near  $q=0.1$ .

wet and dry states overlap. This result confirms previous experimental results [6]. However, notice that the use of small  $q$  values considerably reduces the spread, thus permitting the assessment of each drying state with a single frame. Fig. 4 shows the standard deviation of the 10 measurements in Fig. 3 as a function of  $q$  and the diminishing of the spread can be easily appreciated and a minimum value is registered near  $q=0.1$ .

Choosing this  $q$  value, a measurement of a drying process using single frames and the LASCAq algorithm was processed. As it has already been shown in previous work [6], when the paint is wet the speckle activity is high and it diminishes as the sample drying progresses. As LASCA is a measure of the contrast it can be expected that it should be smaller at the beginning, when the speckle pattern is more blurred and that it should increase with time as paint dries and to achieve its maximum value when the paint is completely dry. It is shown in Fig. 5 that the measured LASCAq ( $q=0.1$ ) value increases as the activity of the sample diminishes with the progressive drying of the sample as could be expected.

*Tsallis q-entropy* was also tested on the same experimental data as in the previous description.

It is to be expected that when the sample is very active: when the paint is wet, the image blurs, the differences between different pixels tend to wash out, most of the pixel intensities tend to similar values, the spatial contrast diminishes and the entropy value tends to be low. Conversely, when the paint is dry, all the images are similar, the contrast of the added images remains high, the histogram of the intensity levels is more evenly populated and the entropy is higher than in the former case. It was found that the use of single frames did not permit very good discrimination between different drying states but the performance notably improved if more than one frame was added.

Fig. 6 shows *Tsallis q entropy* of the wet and dry states of the drying of paint data plotted for different  $q$  values where 8 integrated contiguous frames were used as input to the algorithm. In this case, the measurement was repeated 10 times and the results are plotted together but they can hardly be distinguished because the spread in the measurements is very small. To show the spread, Fig. 7 is a plot of the relative error for those

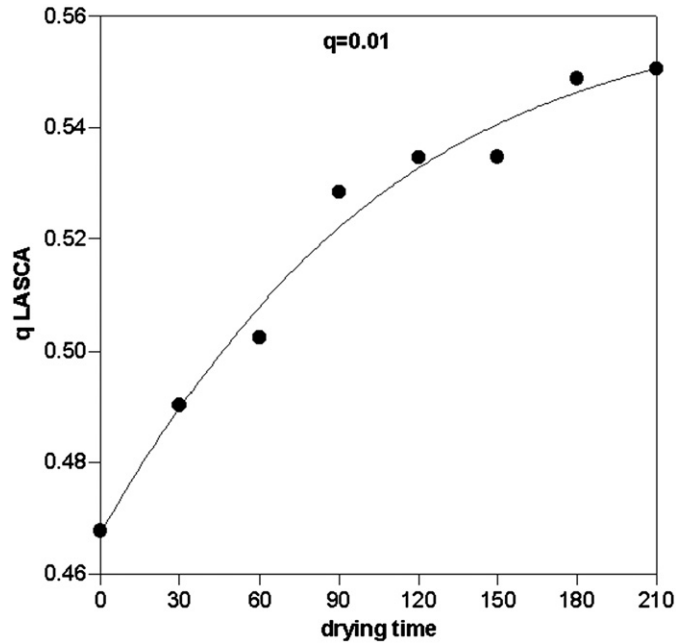


Fig. 5. Drying process using LASCAq for  $q=0.1$ . The measured LASCAq ( $q=0.1$ ) value increases as the activity of the sample diminishes with the progressive drying of the sample.

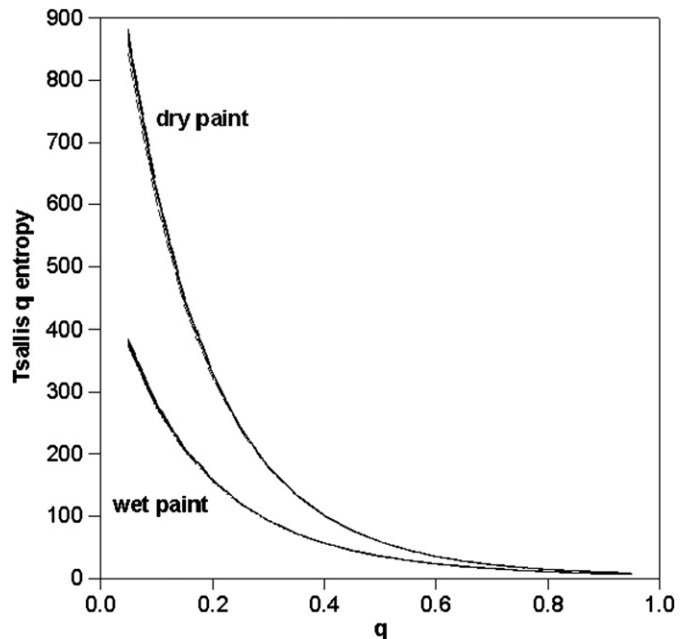


Fig. 6. *Tsallis q entropy* of the wet and dry states of the drying of paint data plotted for different  $q$  values. The measurement was repeated 10 times.

measurements. Notice that even in the worst of cases the relative error is very small.

It can be seen that, even if in Fig. 6 it is not obvious where the measurement shows better discrimination between drying states, it is for  $q$  close to 1 where the relative error is smaller and of the order of 0.1% showing excellent discrimination.

An example of the use of the  $q$  version of the Inertia Moment of the co-occurrence matrix can be seen in Fig. 8 for the drying of paint. The relative error of these measurements can be seen in Fig. 9. In this case,  $q=0.8$  is the value where it is the minimum, but for the other  $q < 1$  values the difference is not very significant (notice the scale of the relative error).

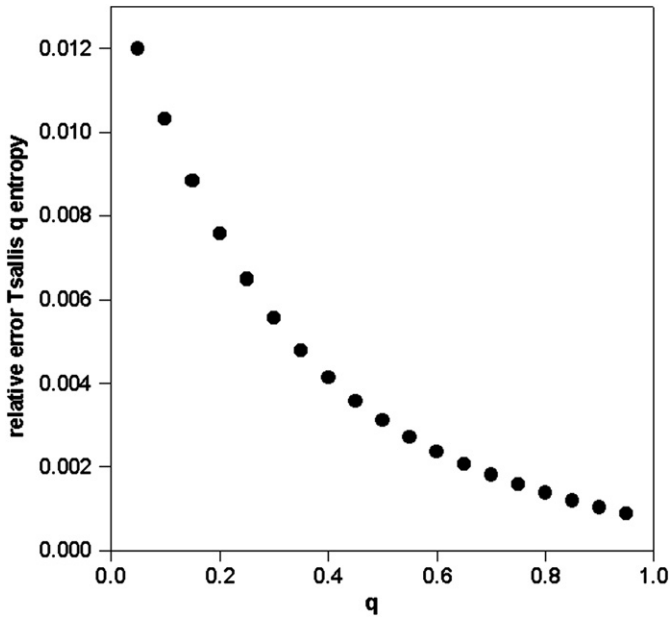


Fig. 7. Relative error of the Tsallis  $q$  entropy for the measurements shown in Fig. 6.

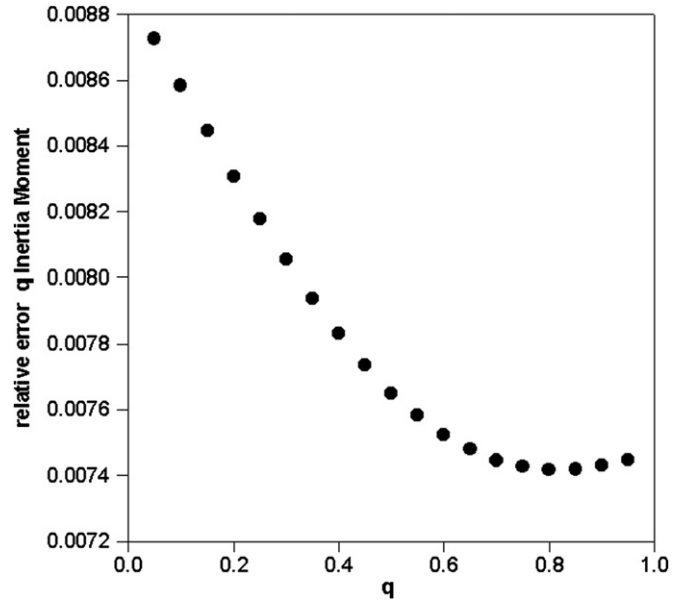


Fig. 9. Relative error of the  $q$  Inertia moment.  $q=0.8$  is the value where it is the minimum; in other  $q < 1$  values, the difference is not very significant.

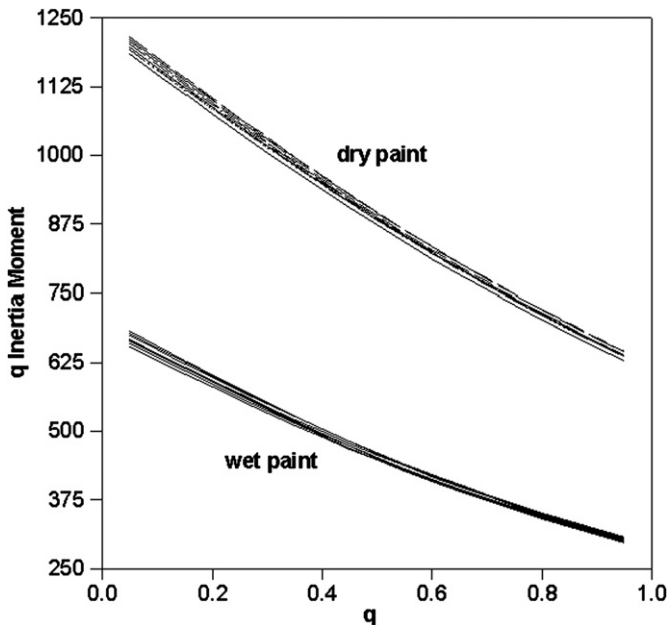


Fig. 8.  $q$  Inertia Moment of the co-occurrence matrix for the drying of paint. Both states are clearly resolved.

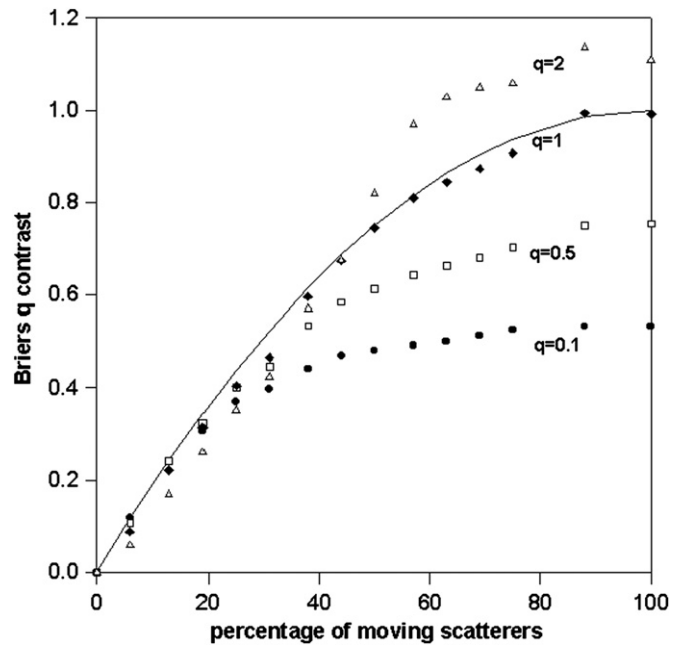


Fig. 10. Briers's temporal contrast of different  $q$  values using numerical simulations for the proportions of moving scatterers. For  $q=1$ , the measurements coincide with the classical theoretical result. For  $q > 1$  the result overshoots the  $q=1$  curve and it is lower for  $q < 1$ .

So, it is evident that for the different measuring methods the value of  $q$  that performs better is different, as for LASCA it is small, for Tsallis  $q$  entropy close to 1 and almost the same value for all the 0, 1 interval when it is the Moment of Inertia  $q$ .

Finally, using Eq. (12) the  $q$  version of Briers's temporal contrast was calculated with different  $q$  values using numerical simulations for the proportions of moving scatterers. When the  $q$  versions of these magnitudes are employed and plotted versus  $\rho$  (see Fig. 10) it is found that for  $q=1$ , of course, the measurements coincide with the classical theoretical result as in Eq. (11). For  $q > 1$  the result overshoots the  $q=1$  curve and is lower for  $q < 1$ . This is not the right physical description but if the proportion of moving scatterers is to be inferred from experimental values of the  $q$  contrast, Fig. 10 shows that when  $q=0.1$  it saturates at  $\rho$  approximately 40% and that for  $q=2$  the plot continues to

increase thus permitting a better discrimination when  $\rho$  is a higher value (up to about 60%).

#### 4. Conclusions

We have explored a generalization of several tools usually used to measure dynamic speckle activity that includes a free parameter  $q$  to change the balance between rare and frequent events in the intensity histogram. We have found that some of them improve their performance when a certain  $q$  value, which depends on the analyzed phenomenon and on the method of measurement, is chosen. Given the wide variety of dynamic

phenomena the approach might not be successful for some of them, but the improvement in the analyzed case was important.

In general, the assessment of the drying of paint process has been characterized with methods that require the processing of many frames. Drying of paint measured using LASCA $q$ , for example, when used with small  $q$  values shows a notorious improvement in resolution and could permit the following of the drying process by using single frames so that it could be followed in almost real time.

The Tsallis entropy requires in this case the integration of 8 frames, thus requiring a somewhat longer acquisition time; but a high discrimination is obtained as a trade.

The moment of inertia of the  $q$  version of the co-occurrence matrix, involving longer acquisition and processing times, did not show any noticeable improvement for the tested  $q$  values.

Besides, the choice of the  $q$  value that optimizes a measure of the activity with respect to some criterion could be eventually be used as a descriptive feature of the involved dynamics. The study of the degree of non-extensivity  $q$  as a descriptor in itself of the dynamics is deferred to a further work. Other phenomena, for example using activity images by dynamic speckle segmentation by  $q$  statistic will be also explored.

### Acknowledgments

This work was supported by CCT La Plata Consejo Nacional de Investigaciones Científicas y Técnicas (CONICET), Comisión de

Investigaciones Científicas de la Provincia de Buenos Aires, by Facultad de Ingeniería, University of La Plata and by a Grant PICT 2008-1430, Agencia Nacional de Promoción de la Ciencia y la Técnica, Argentina. We are grateful to J.I. Amalvy and C. Lasquibar for their valuable assistance in the paint experiments.

### References

- [1] Tsallis C. Possible generalization of Boltzmann–Gibbs statistics. *J Status Phys* 1988;52:479–87.
- [2] Salinas S, Tsallis C. Nonextensive Statistical Mechanics and Thermodynamics. *Br J Phys* 1999;29(1). [special issue ].
- [3] Boon JP, Tsallis C. Nonextensive statistical mechanics: new trends, new perspectives. *Europhys. News* 2005;36(6). [special issue and directory].
- [4] Sirohi RS. *Speckle Metrology*. New York: Academic; 1993.
- [5] Aizu Y, Asakura T. In: Consortini A, editor. *Bio-speckles in Trends in Optics*. London: Academic Press; 1996. [Chapter 2].
- [6] Amalvy JI, Lasquibar CA, Arizaga R, Rabal H, Trivi M. Application of dynamic speckle interferometry to the drying of coatings. *Prog Org Coat* 2001;42:89–99.
- [7] Rabal H, Braga R. *Dynamic Laser Speckle and Applications*. Boca Raton, FL, USA: CRS Press, Taylor and Francis Publisher; 2009.
- [8] Briers JD, Webster S. Laser speckle contrast analysis (LASCA): a non scanning, full field technique for monitoring capillary blood flow. *J Biomed Opt* 1996;1:174–9.
- [9] Briers JD, Richards G, He XW. Capillary blood flow monitoring using laser speckle contrast analysis (LASCA). *J Biomed Opt* 1999;4:164–75.
- [10] Arizaga R, Trivi M, Rabal HJ. Speckle time evolution characterization, by the cooccurrence matrix analysis. *Opt Laser Technol* 1999;31:163–9.
- [11] Briers JD. The statistics of fluctuating speckle patterns produced by a mixture of moving and stationary scatterers. *Opt Quantum Electron* 1978;10:364–6.
- [12] Sendra GH, Rabal H, Trivi M, Arizaga R. Numerical model for simulation of dynamic speckle reference patterns. *Opt Commun* 2009;282:3693–700.